

Supporting Information

Layered Zinc Hydroxide Monolayers by Hydrolysis of Organozincs

Alice. H. M. Leung,^a Sebastian D. Pike,^a Adam J. Clancy,^a Hin Chun Yau,^a Won Jun Lee,^a

Katherine L. Orchard, Milo S. P. Shaffer,^{*ab} Charlotte K. Williams^{*ac}

^a *Department of Chemistry, Imperial College London, London, UK. SW7 2AZ.*

^b *Department of Materials, Imperial College London, London, UK. SW7 2AZ.*

^c *Chemistry Research Laboratory, University of Oxford, 12 Mansfield Road, Oxford, UK. OX1 3TA.*

Corresponding author email: c.k.williams@imperial.ac.uk and m.shaffer@imperial.ac.uk

Index

Page 1–2	Table S1–S4
Page 3–13	Figure S1–S18
Page 14–16	Determining the content of ZnO nanoparticles in synthesis mixture
Page 17	Determining yield of LZHS
Page 17	References

Carboxylate loading [COOR]/[Zn]	Molar Ratio of ZnEt ₂ :Zn(COOR) ₂	Moles of ZnEt ₂ / mmol	Moles of Zn(COOR) ₂ / mmol
0.40	4:1	1.093	0.273
0.50	3:1	1.024	0.342
0.60	2.3:1	0.952	0.414

Table S1. Table showing the corresponding molar ratios and moles of ZnEt₂ and Zn(COOR)₂ required for the synthesis of LZH at different carboxylate loading.

LZH	Basal plane	°2θ	Spacing/ Å
OAc	(001)	6.3	14.1
	(002)	12.6	7.0
	(003)	18.9	4.7
OHex	(001)	3.9	22.7
	(002)	7.7	11.5
	(003)	11.5	7.7
	(004)	15.4	5.8
	(005)	19.2	4.6
Ole	(001)	1.92	45.9 ± 0.8
	(002)	4.0	22.1
	(003)	5.8	15.2
	(004)	7.6	11.6
	(005)	9.3	9.5

Table S2. Table showing the spacing for each basal planes of LZH-OAc, LZH-OHex and LZH-Ole. For LZH-Ole, the spacing for (001) is predicted from the (002), (003), (004) and (005) peaks, as the (001) was not observed in XRD pattern (the peak lies beyond the limits of the diffractometer).

LZH	Expected wt% C ^a	wt% C (from TGA)	wt% C (from elemental analysis)
LZH-OAc	11.26	10.53	12.72
LZH-OHex	26.74	23.72	27.25
LZH-Ole	49.61	49.73	49.39

^a expected wt% C calculated from the chemical formula: $[Zn_5(OH)_8(COOR)_2]$ with excess ligand taken into account.

Table S3. Table showing the %C obtained for LZH-OAc, LZH-OHex and LZH-Ole, synthesised using $[COOR]/[Zn] = 0.60$, from thermogravimetric analysis and elemental analysis. For the %C from TGA data, the carbon loss is entirely attributed to the second mass-loss observed (see Figs. S9, S10).

Solvent	Solubility (mg/mL)
Toluene	23
Hexane	5
Chloroform	14
Dichloromethane	2
Ethanol	0
Water	0

Table S4. Table showing the solubility of LZH-Ole in different solvents.

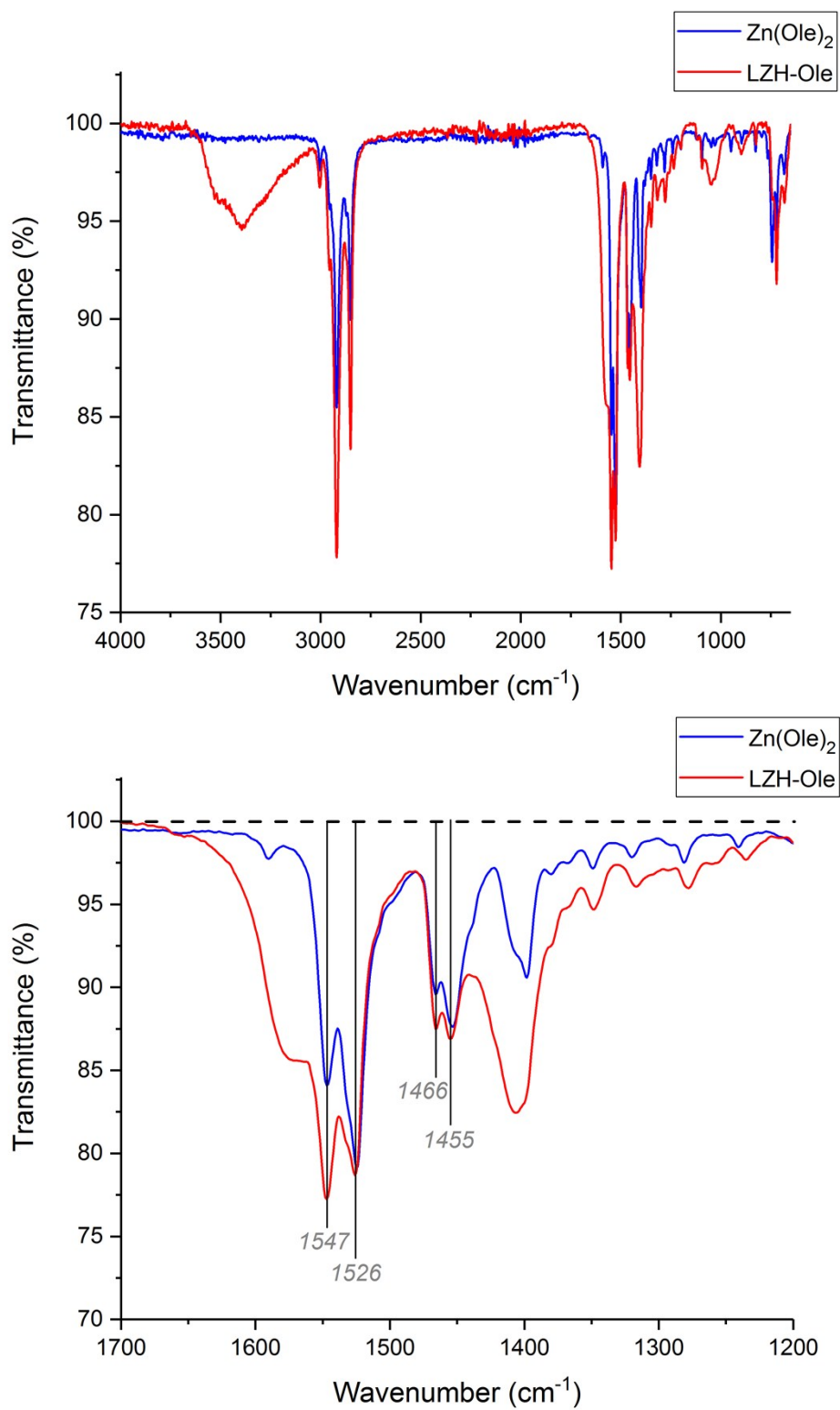


Figure S1. (Top) A comparison of IR spectra of LZH-Ole with Zn(Ole)₂ and (bottom) zoomed spectra in the region of carboxylate C–O stretches.

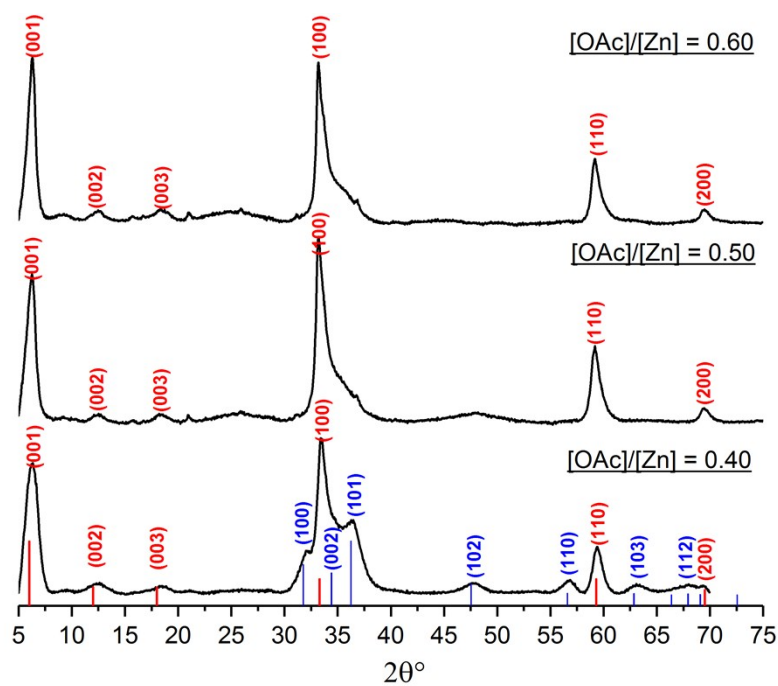


Figure S2. Stack XRD patterns of products from different loading of acetate within the synthesis mixture. [OAc]/[Zn] = 0.40 shows the presence of ZnO nanoparticles along with LZH-OAc. Reference data: LZH-OAc (red) reported by Poul *et al.*¹, ZnO (blue, JCPDS card no.: 00-001-1136).

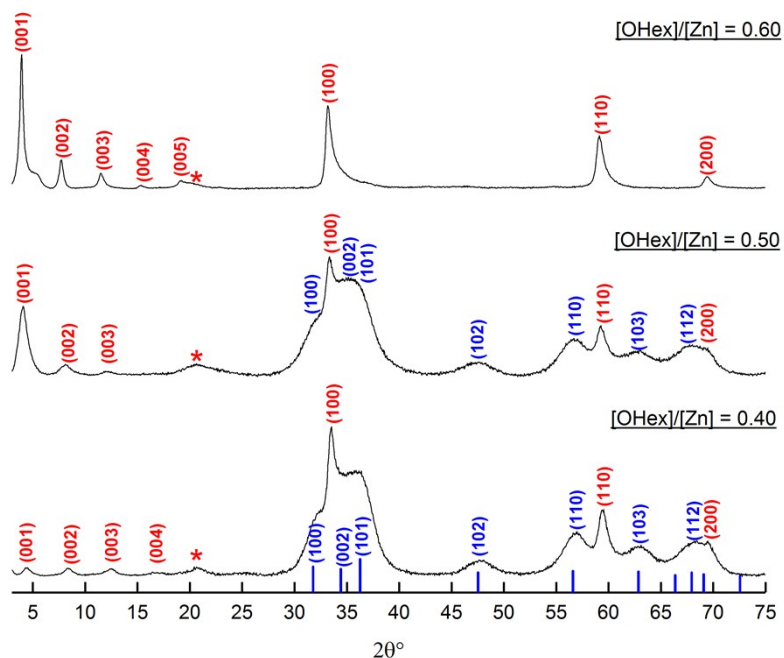


Figure S3. Stack XRD patterns of products from different loading of hexanoate within the synthesis mixture. [OHex]/[Zn] = 0.40 and 0.50 show the presence of ZnO nanoparticles along with LZH-OHex. Reference data: ZnO (blue, JCPDS card no.: 00-001-1136).

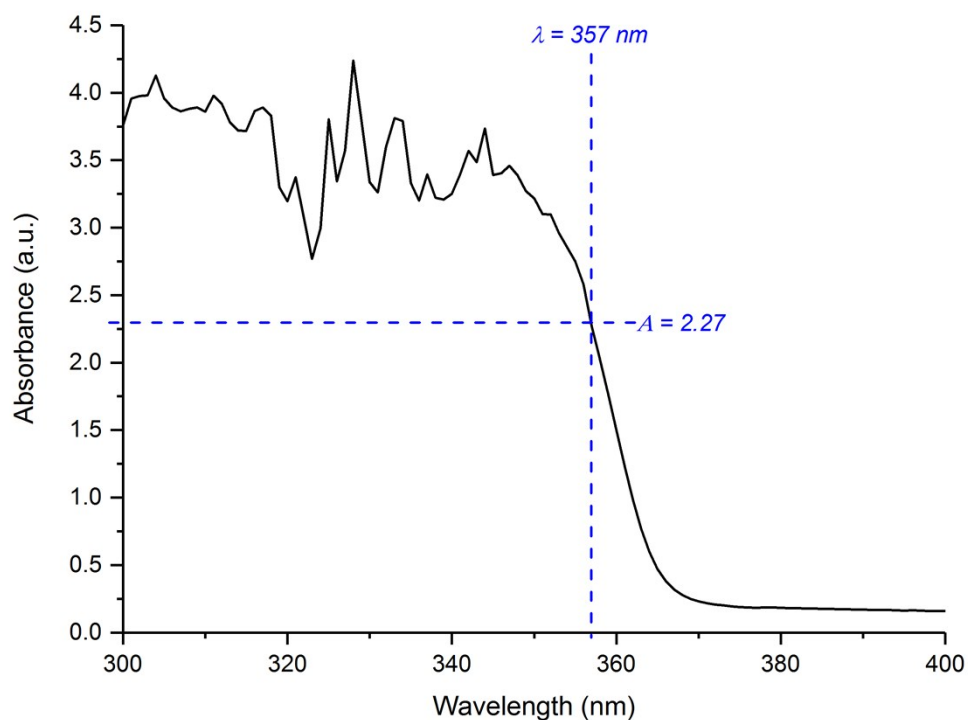


Figure S4. The UV-Vis spectrum of solution of reaction mixture for the synthesis of LZH-Ole. The blue dashed lines identify the point used to estimate the ZnO concentration, by comparison to the calibration curve in Figure S21.

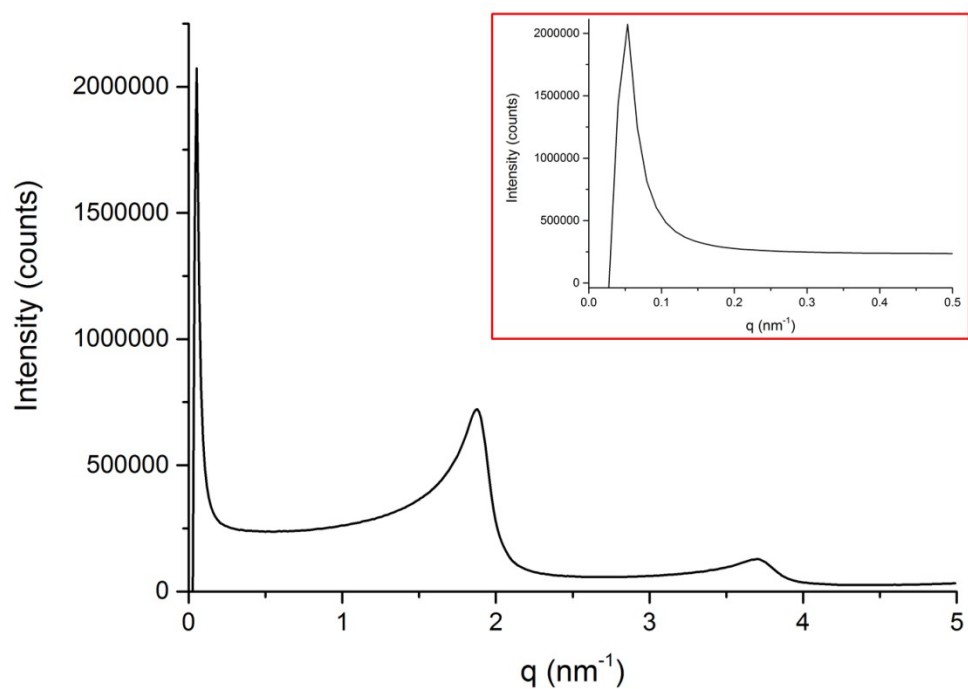


Figure S5. Solid-state SAXS spectrum of LZH-Ole with the inset showing the part of the spectrum where the volume-weighted size distribution ($D_v(R)$) calculation was taken.

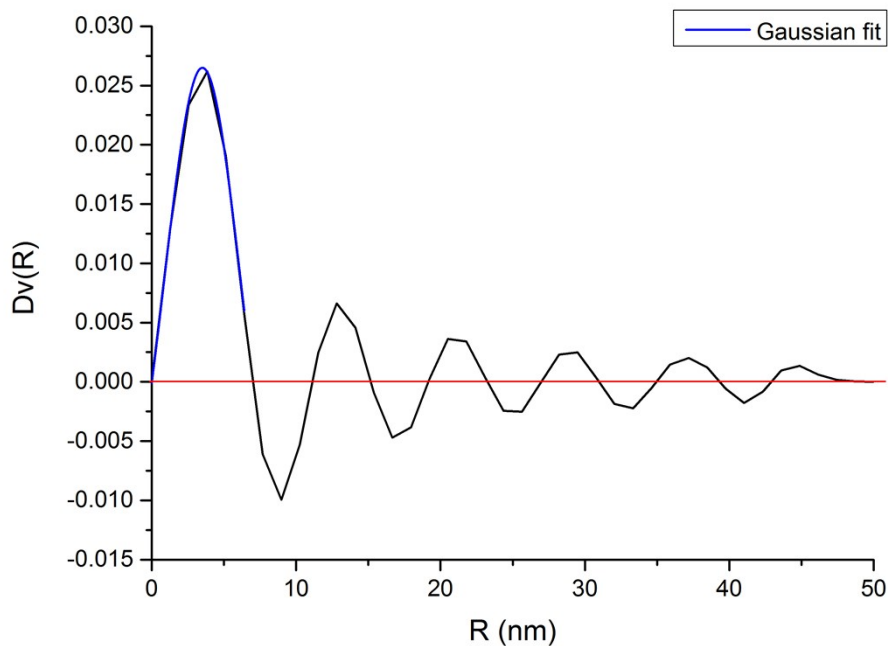


Figure S6. Graph showing the interlayer distance, R , against the volume-weighted size distribution, $D_v(R)$, for LZH-Ole, where a Gaussian curve fit is applied to the first and most populated peak, corresponding to the (001) plane. The most frequent R is 3.85 nm and the subsequent peaks >10 nm are caused by the long range stacking of the material. $D_v(R)$ was calculated through performing indirect Fourier transform on the intensity values obtained from SAXS measurement, using EasySAXS software.

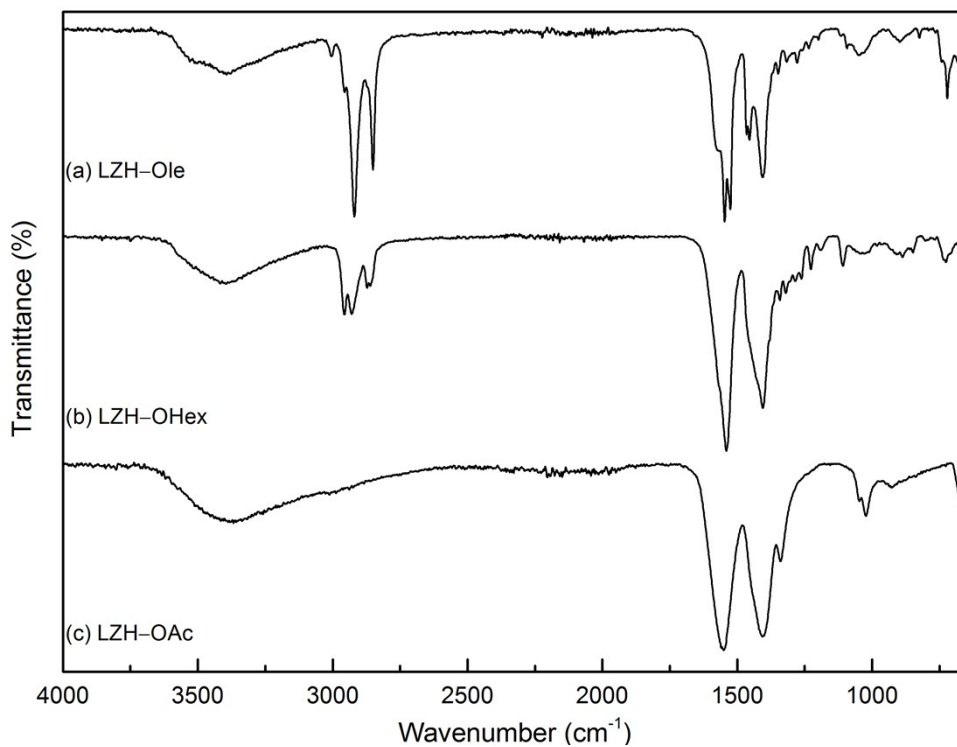


Figure S7. IR spectra of (a) LZH-Ole, (b) LZH-OHex and (c) LZH-OAc.

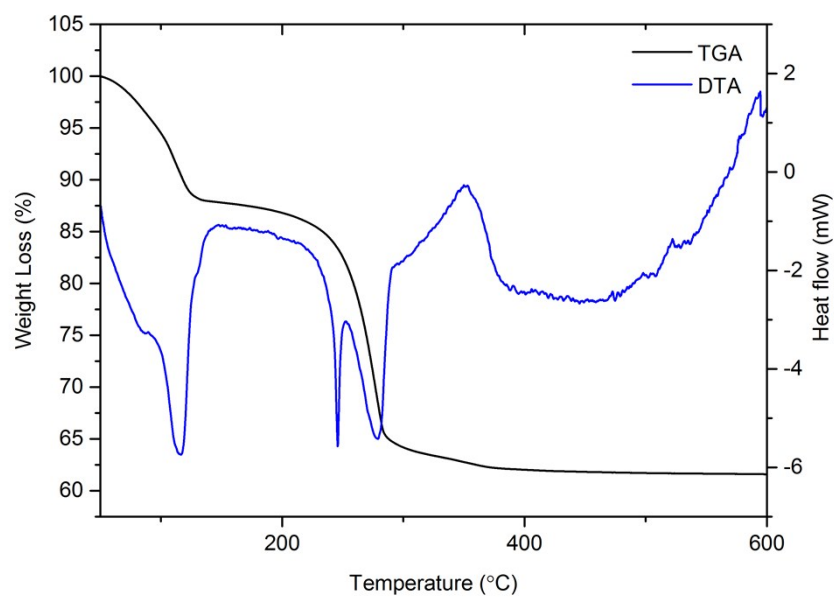


Figure S8. TGA and DTA profile of LZH-OAc from 50–600°C, under a flow of synthetic air with a heating rate of 5°C/min.

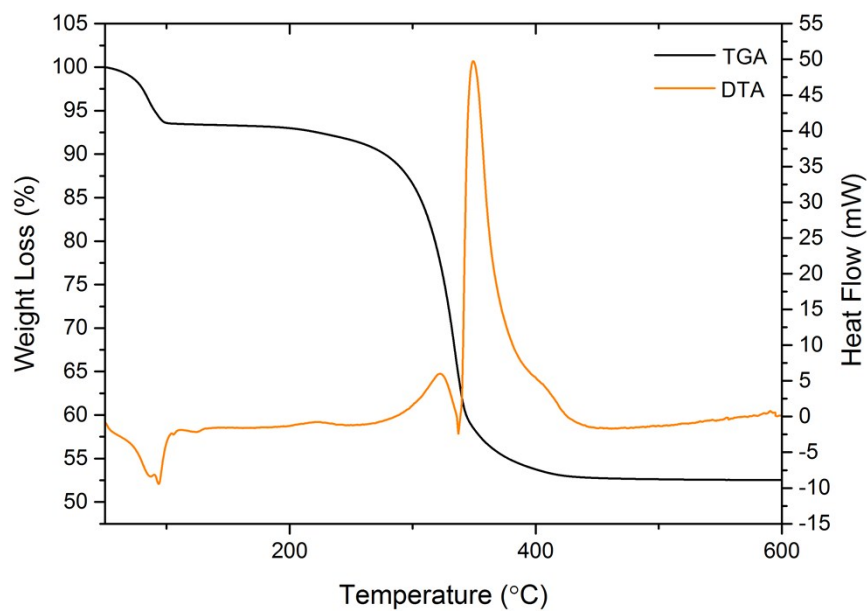


Figure S9. TGA and DTA profile of LZH-OHex from 50–600°C, under a flow of synthetic air with a heating rate of 5°C/min.

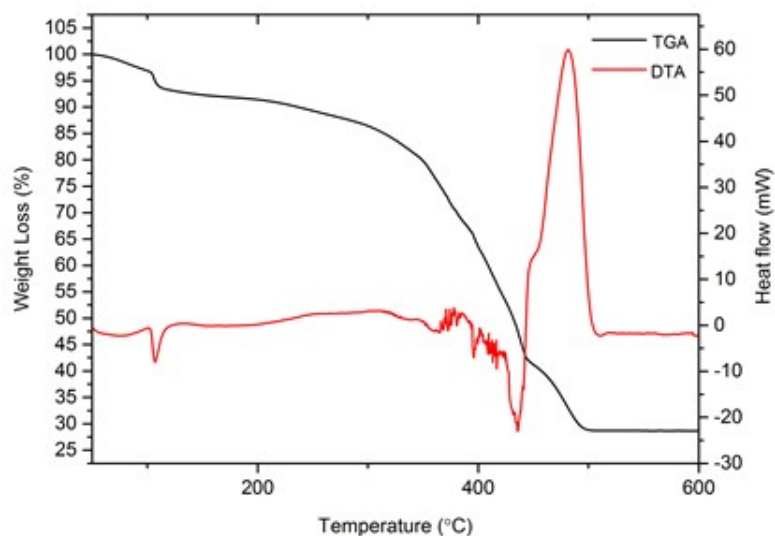


Figure S10. TGA and DTA profile of LZH-Ole from 50–600°C, under a flow of synthetic air with a heating rate of 5°C/min.

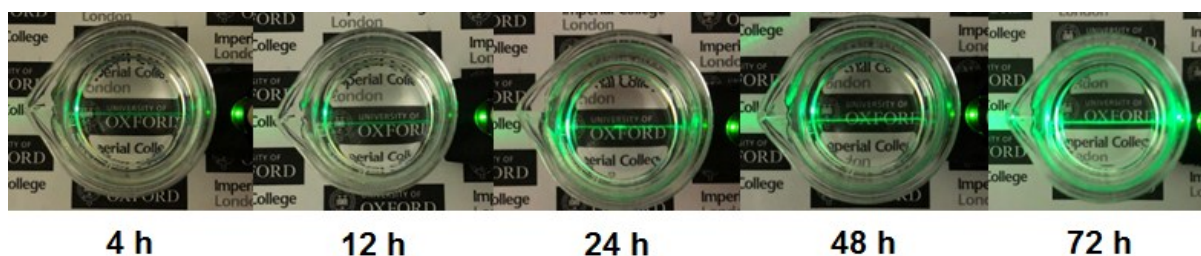


Figure S11. Photographs showing the spontaneous dissolution of LZH-Ole in toluene, over a period of 72 h. The increasing concentration of nanoplatelets is revealed by Rayleigh scattering from an incident laser beam which becomes stronger over time as more LZH dissolves., although the solution remains transparent.

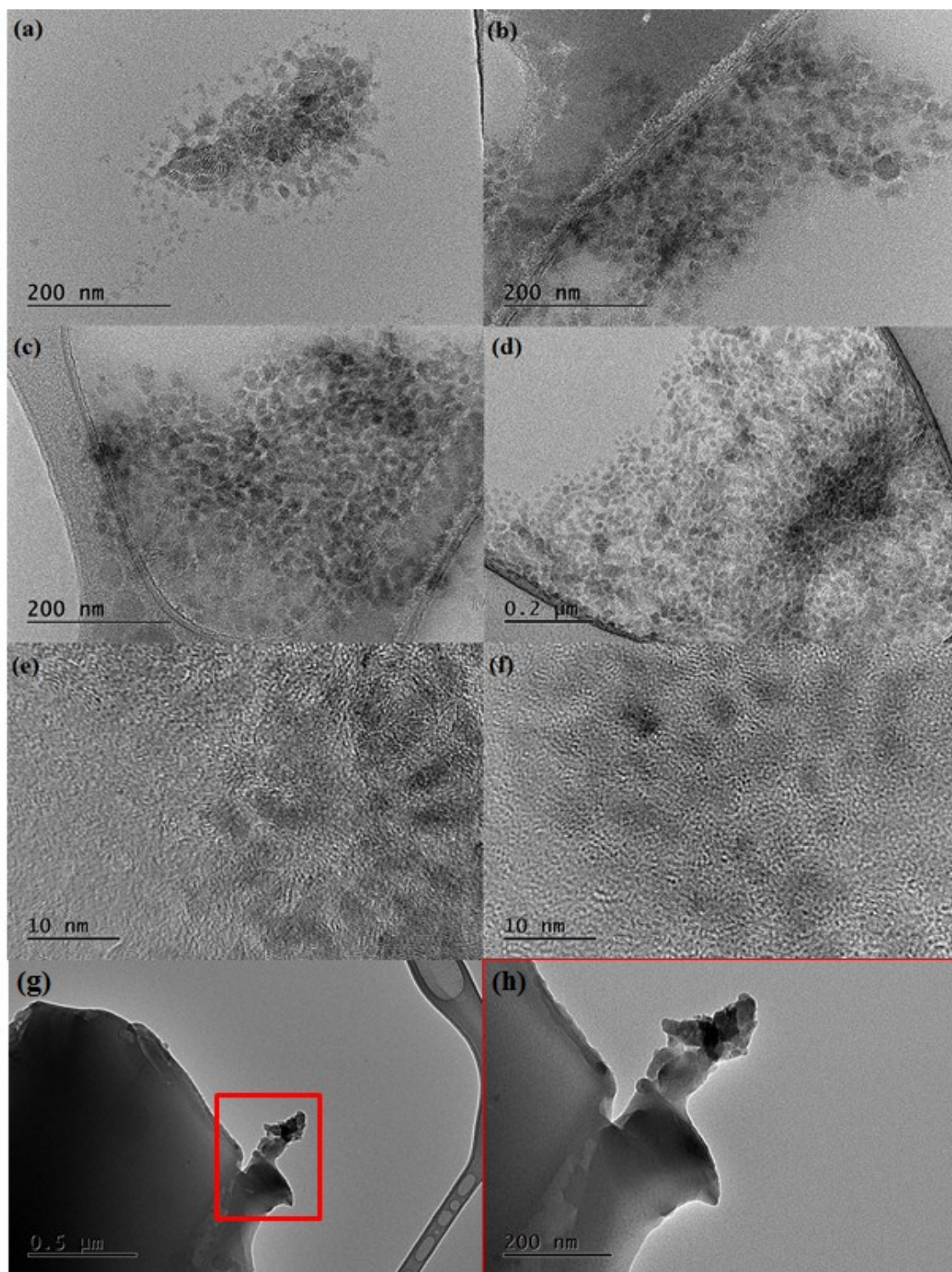


Figure S12. (a)–(d) TEM images showing the agglomeration of nanoplatelets of LZH-Ole after exfoliation (in toluene, mechanical stirring, 2 h). The sizes of the agglomerates varied from 0.4–1 μm , with the densest section (darkest regions in bright field TEM image mode) being in the middle of agglomerates with thin nanoplatelets on the edge of agglomerates. (e)–(f) HRTEM of the edges of agglomerates of LZH-Ole. (g) TEM image of the unexfoliated LZH-Ole sample (bulk sample briefly shaken in toluene without allowing time for dissolution) with (h) showing higher magnification of the red box highlighted in (g).

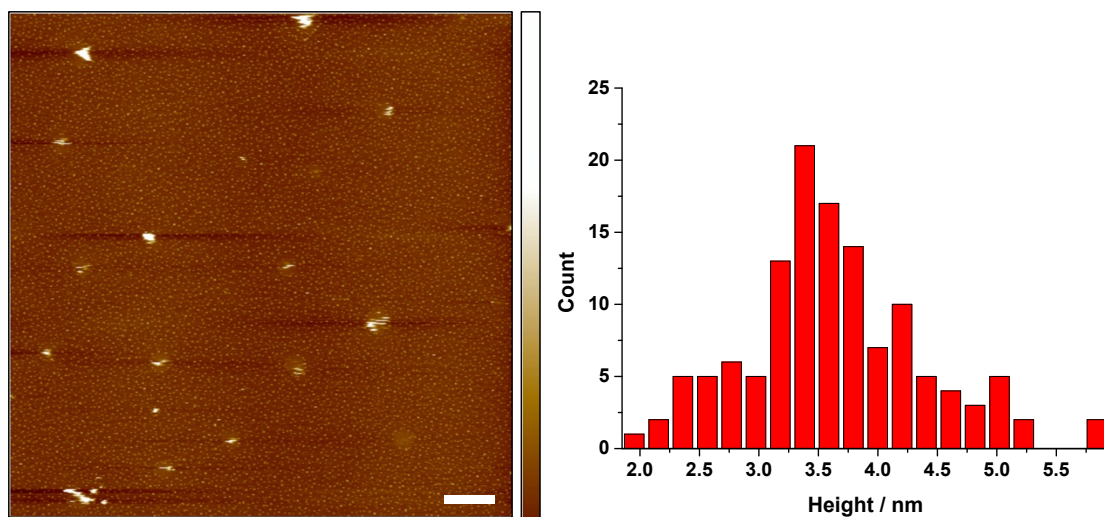


Figure S13. (Left) Large area AFM image of LZH-Ole and (Right) height distribution of the individual platelets ($N = 127$, mean 3.628 ± 0.748 nm). Scale bars: horizontal : $1 \mu\text{m}$, vertical : 10 nm.

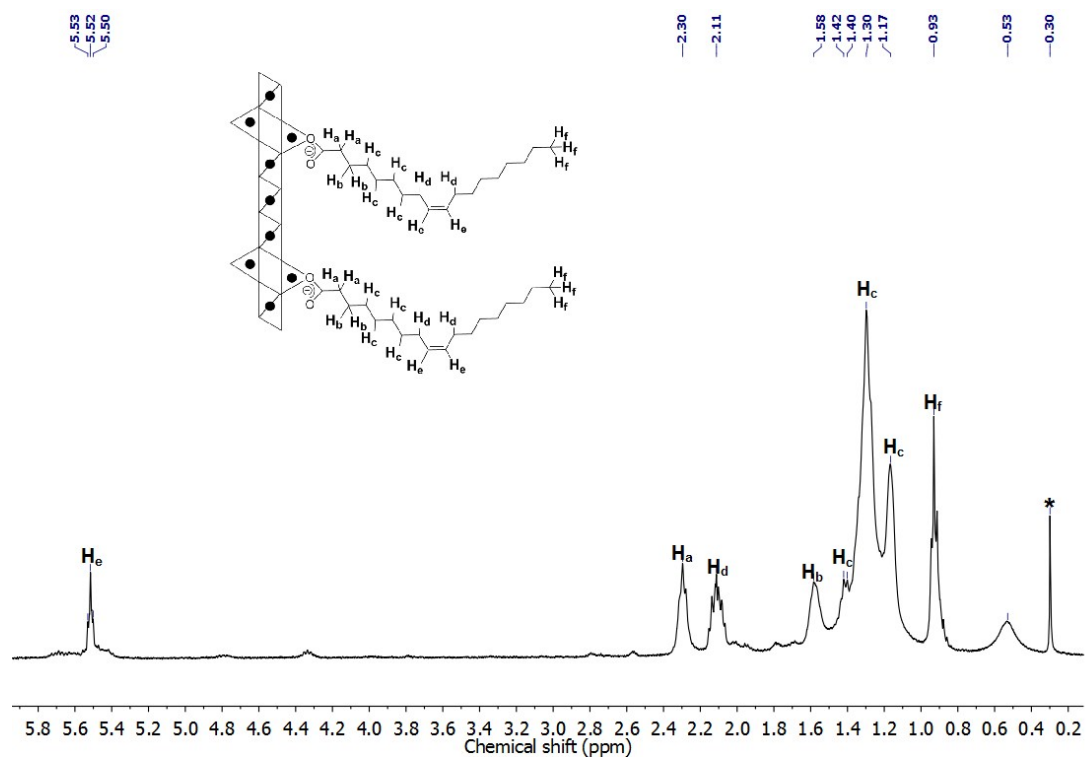


Figure S14. ^1H NMR spectrum of LZH-Ole in C_6D_6 .

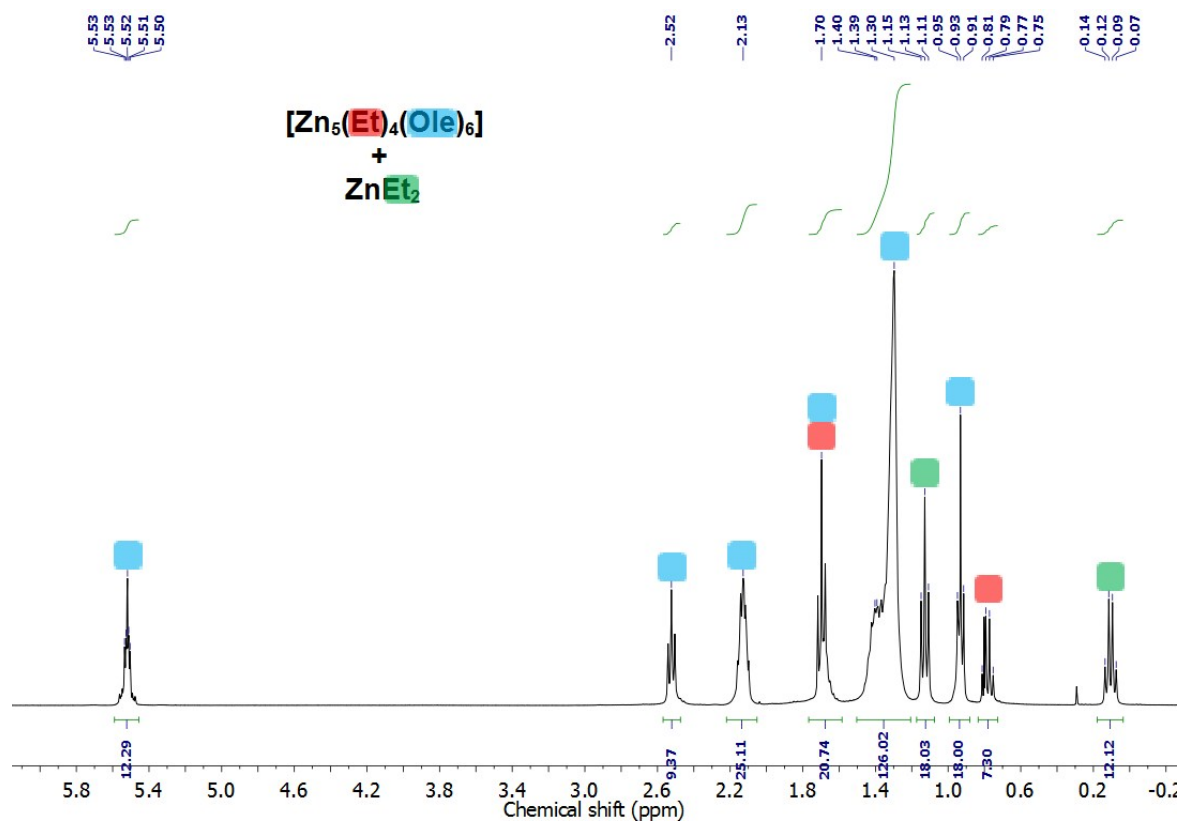


Figure S15. 1H NMR spectrum of pre-hydrolysis mixture, in C_6D_6 , containing free $ZnEt_2$ and pentanuclear complex, $[Zn_5(Et)_4(Ole)_6]$, which has the same structure as $[Zn_5(Et)_4(OAc)_6]$ reported by K. Orchard *et al.*²

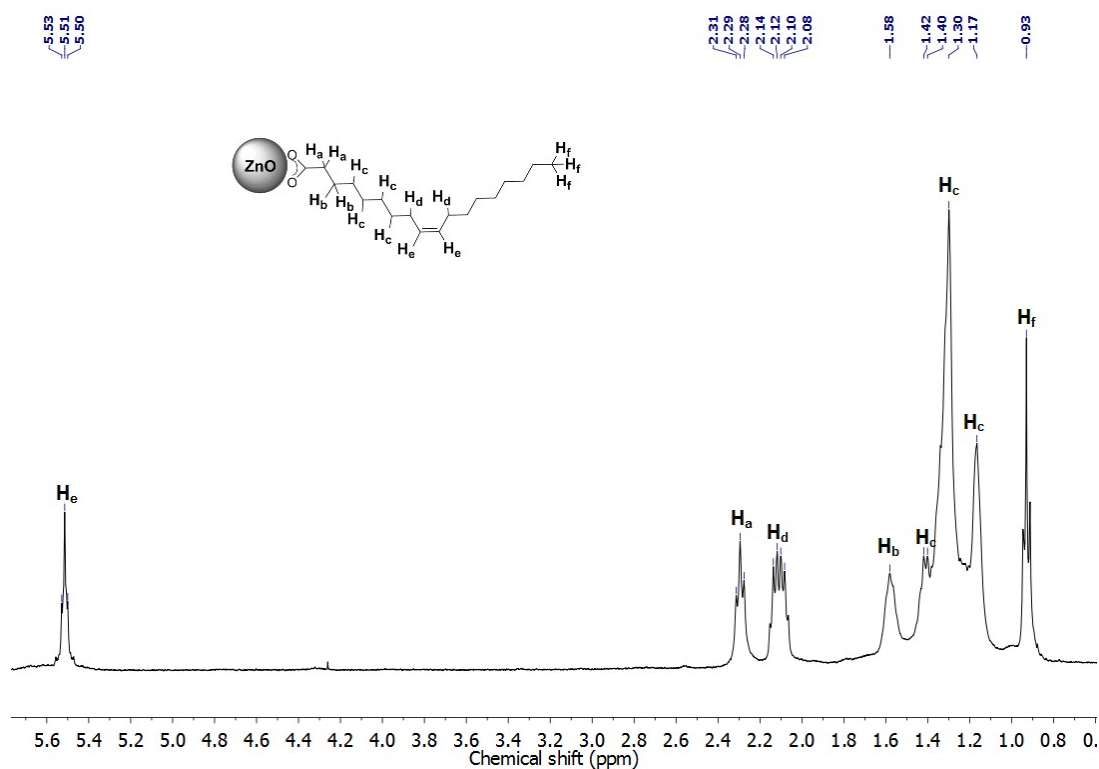


Figure S16. 1H NMR spectrum of $ZnO@Ole$ nanoparticles in C_6D_6 .



Figure S17. Photographs of (*left*) LZH film on glass substrate and (*right*) a transparent ZnO film on glass substrate formed by annealing a film of LZH-Ole at 500°C for 15 mins under air.

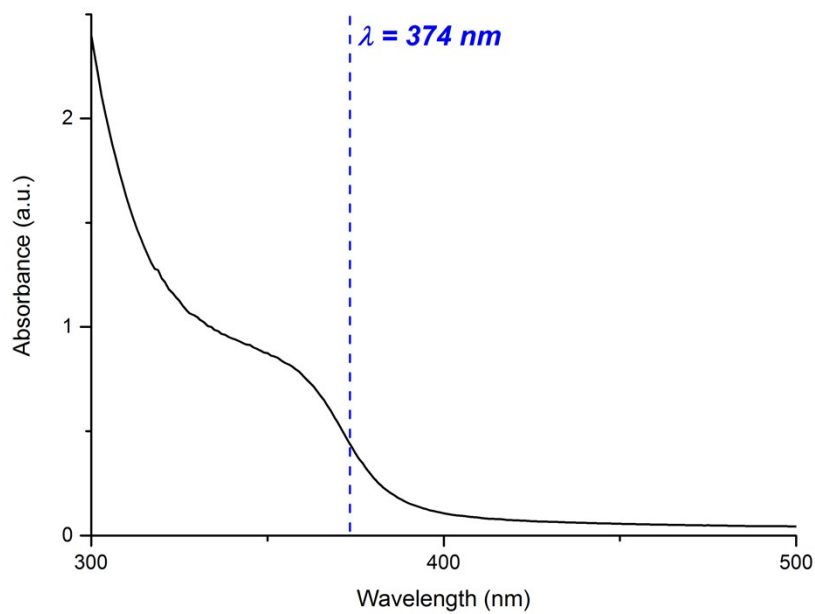


Figure S18. UV-Vis spectrum of annealed ZnO film on glass substrate after thermal treatment of 500°C for 15 mins under air.

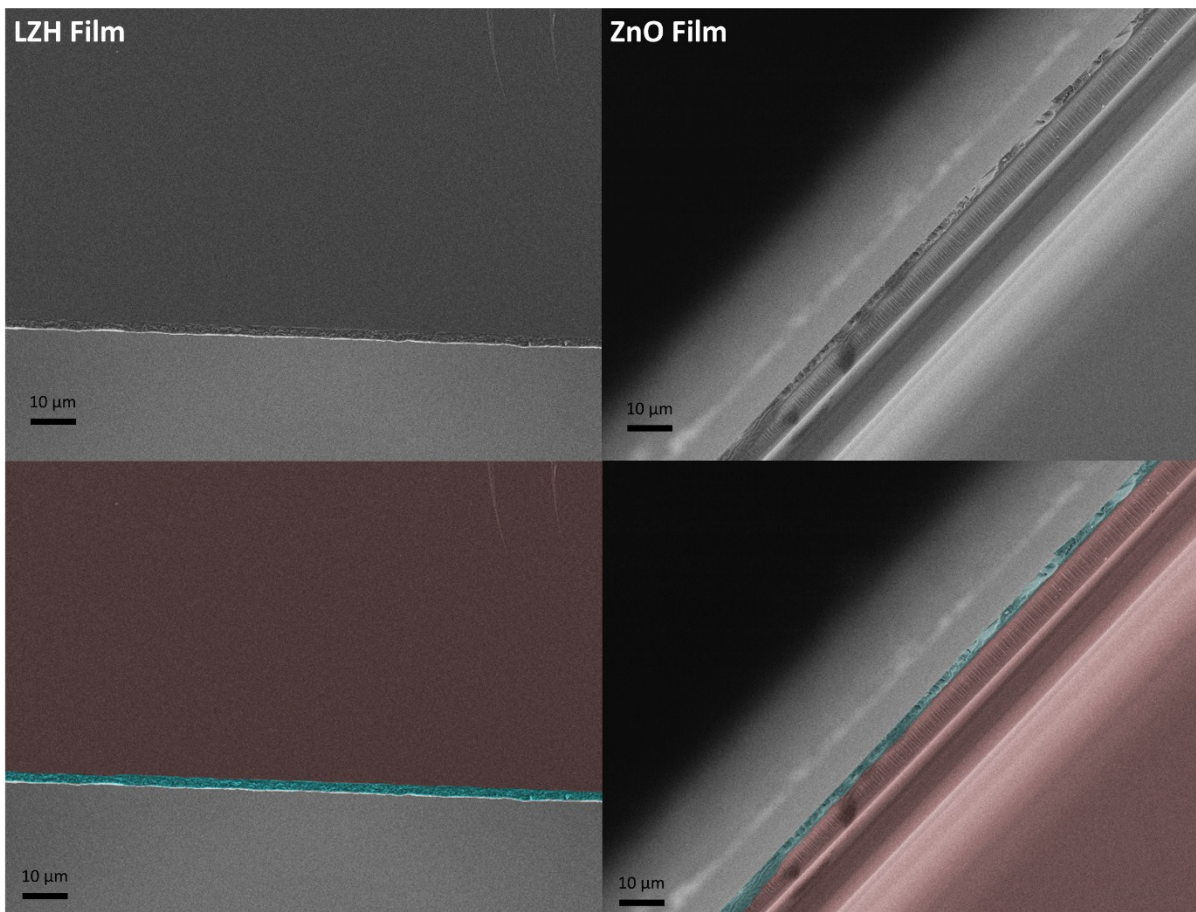


Figure S19. SEM images of the (top) cross sections of LZH film and ZnO film. False colour added to the same SEM images (bottom) highlights the even thickness of the deposited LZH and ZnO film (blue) on glass (red).

Determining the content of ZnO nanoparticles in synthesis mixture

The optical absorbance of oleate-capped ZnO nanoparticles (ZnO@Ole) in toluene was calibrated by systematic UV-Vis spectroscopy as a function of concentration. The ZnO@Ole was synthesised by thermal decomposition of LZH-Ole ([Ole]/[Zn] = 0.60) *in vacuo* at 60°C for 2 h and the material was confirmed to be ZnO nanoparticles by powder XRD (figure S19). The approach was used to ensure that the calibration standard was well matched to the LZH samples under study. Known quantities of ZnO@Ole were dissolved in toluene (9.11 mL), and the ZnO concentration calculated using the experimental elemental analysis data (%C 46.64), to obtain a series of UV-vis spectra (Figure S21, top). To allow direct monitoring of the experimental reaction mixtures, without dilution, the extinction coefficient was calculated at $\lambda = 357$ nm to avoid saturation effects (Figure S21, bottom). The extinction coefficient (ϵ) of ZnO nanoparticles was determined to be $755 \text{ dm}^2 \text{ mol}^{-1}$ at $\lambda = 357$ nm. For comparison to literature³, the extinction coefficient was also calculated at $\lambda = 325$ nm; the ϵ value of $31.9 \text{ m}^2 \text{ mol}^{-1}$ for ZnO@Ole is in good agreement with literature ($\epsilon = 30\text{--}45 \text{ m}^2 \text{ mol}^{-1}$) in this range. This reference also highlights a relatively weak effect of size on extinction coefficient in the narrow size range expected for ZnO produced via the organometallic route (3-4 nm).

The reaction mixture from the synthesis of LZH-Ole (containing 1.366 mmol Zn in total) was analysed by UV-Vis spectroscopy in the same way. Since the optical absorbance of LZH is negligible in this range, the content of ZnO was determined by the absorbance at $\lambda = 357$ nm, which is equal to the concentration of 0.0300 M (i.e. 0.274 mmol, or 20 mol% Zn, in the sample).

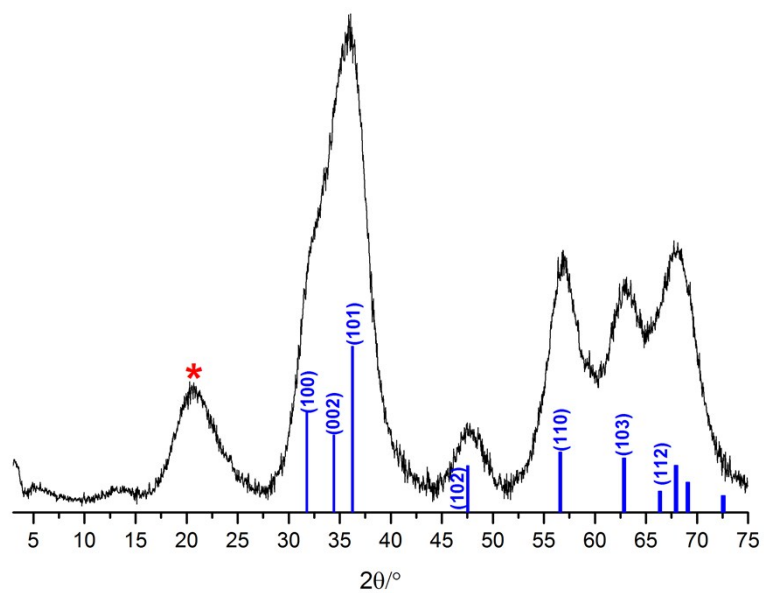


Figure S20. The XRD pattern of ZnO@Ole synthesised from thermal decomposition of LZH-Ole *in vacuo* at 60°C for 2 h. The peak highlighted by '*' is caused by the hydrocarbon chains of oleate/oleic acid. Reference data: ZnO (blue, JCPDS card no.: 00-001-1136).

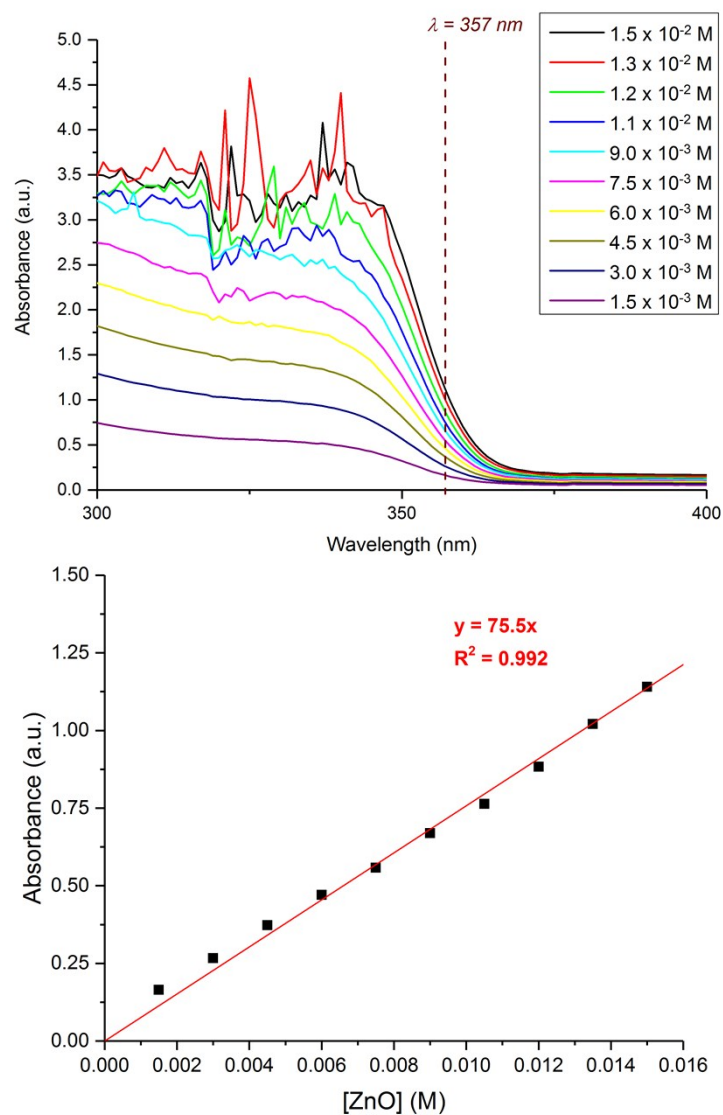


Figure S21. (Top) The combined UV-Vis spectra (path length 0.1 dm) for the standards of ZnO@Ole (in toluene) with the wavelength marked where the absorbance readings were taken. (Bottom) The calibration plot showing the linear relationship between the concentration of Zn (as ZnO) in toluene and absorbance.

Determining the yield of Ole-LZH

For a synthesis containing 1.366 mmol of Zn and 0.8196 mmol COOR (1:0.6) in total, UV-Vis spectroscopy (above) shows that 20 mol% is in the form of ZnO. Assuming that the remaining Zn (1.093 mmol) are incorporated as $x [\text{Zn}_5(\text{OH})_8(\text{COOR})_2] + y \text{Zn}(\text{COOR})_2$ two constraints apply:

from Zn balance:

$$5x + y = 1.093 \quad (1)$$

and COOR balance:

$$2x + 2y = 0.8196 \quad (2)$$

Solving these simultaneous equations indicates that there are 0.854 mmol of Zn in LZH, and 0.239 mmol of Zn in $\text{Zn}(\text{COOR})_2$, hence the molar yield of LZH-Ole is 62.5 mol% Zn, and the mass content of ZnO is 6.4 wt%.

Species in products	Molar proportions/ mol% Zn	Mass per Zn/ mg	Mass proportions in product/ mg	wt% in product
LZH-Ole ^a	62.5	205.1	128.2	50.4
$\text{Zn}(\text{Ole})_2$	17.5	627.3	109.8	43.2
ZnO	20.0	81.3	16.3	6.4

^a chemical formula of $[\text{Zn}_5(\text{OH})_8(\text{COOR})_2]$

Table S5. Table showing the estimation of ZnO wt% in the final product from LZH-Ole synthesis.

References

1. L. Poul, N. Jouini and F. Fiévet, *Chem. Mater.*, 2000, **12**, 3123-3132.
2. K. L. Orchard, A. J. P. White, M. S. P. Shaffer and C. K. Williams, *Organometallics*, 2009, **28**, 5828-5832.
3. D. Segets, J. Gradl, R. K. Taylor, V. Vassilev and W. Peukert, *ACS nano*, 2009, **3**, 1703-1710.